

International Journal of Modern Physics A  
 © World Scientific Publishing Company

## THERMODYNAMICS OF NJL-LIKE MODELS

FRIESEN A.V.

*Bogoliubov Laboratory of Theoretical Physics, Joint Institute for Nuclear Research, 141980  
 Dubna, Russia  
 avfriesen@theor.jinr.ru*

KALINOVSKY Yu.L.

*Laboratory of Information Technologies, Joint Institute for Nuclear Research, 141980 Dubna,  
 Russia  
 Higher Mathematics Department, University "Dubna", Dubna, Russia  
 kalinov@jinr.ru*

TONEEV V.D.

*Bogoliubov Laboratory of Theoretical Physics, Joint Institute for Nuclear Research, 141980  
 Dubna, Russia  
 toneev@theor.jinr.ru*

Received Day Month Year

Revised Day Month Year

The thermodynamic behavior of conventional Nambu–Jona-Lasinio and Polyakov-loop-extended Nambu–Jona-Lasinio models is compared. Particular attention is paid to the phase diagram in the  $T - \mu$  plane.

*Keywords:* NJL model; PNJL model; phase diagram

PACS numbers: 11.30.Rd, 12.20.Ds, 14.40.Be

### 1. Introduction

Models of the Nambu–Jona-Lasinio (NJL) type <sup>1,2</sup> have a long history and have been extensively used to describe the dynamics of lightest hadrons and the thermodynamic properties of excited matter (see the review articles <sup>3,4,5,6,7</sup>). In the “classical” versions such schematic models incorporate the chiral symmetry of two-flavor QCD and its spontaneous breakdown at temperatures below the critical one,  $T < T_c$ . They offer a simple and practical illustration of the basic mechanisms that drive the spontaneous breaking of chiral symmetry, a key feature of QCD in its low-temperature, low-density phase. However, in spite of their widespread use, the NJL models suffer from the major shortcoming that the reduction to global color symmetry prevents quark confinement.

In the Polyakov-loop-extended NJL (PNJL) model <sup>8–12</sup>, the quarks are coupled simultaneously to the chiral condensate, to be an order parameter of the chi-

ral symmetry breaking, and to a homogeneous gauge field representing Polyakov loop dynamics, which serves as an order parameter for the transition from the low-temperature, symmetric, confined phase to the high-temperature, deconfined phase. The model has proven successful in reproducing lattice data on QCD thermodynamics<sup>10</sup>.

In this paper we confront general properties of  $\pi$  and  $\sigma$  mesons as well as thermodynamics at finite temperature  $T$  and baryon chemical potential  $\mu$  calculated within the two-flavor NJL model with those of the PNJL one.

### 1.1. Nambu–Jona-Lasinio model

To describe the coupling between quarks and the chiral condensate in the scalar-pseudoscalar sectors, the two-flavor NJL model<sup>1,6,13,14</sup> is used with the following Lagrangian density

$$\mathcal{L}_{\text{NJL}} = \bar{q} (i\not{\partial} - \hat{m}_0) q + G \left[ (\bar{q}q)^2 + (\bar{q}i\gamma_5 \vec{\tau}q)^2 \right], \quad (1)$$

where  $G$  is the coupling constant,  $\vec{\tau}$  is the vector of Pauli matrices in flavor space,  $\bar{q}$  and  $q$  are the quark fields (color and flavor indices are suppressed),  $\hat{m}_0$  is the diagonal matrix of the current quarks masses,  $\hat{m}_0 = \text{diag}(m_u^0, m_d^0)$ ,  $m_u^0 = m_d^0 = m_0$ .

The grand canonical thermodynamic potential can be obtained from this Lagrangian in systematic approximations. In the mean-field approximation it has the form<sup>13</sup>

$$\Omega_{\text{NJL}} = G \langle \bar{q}q \rangle^2 + \Omega_q, \quad (2)$$

with

$$\Omega_q = -2N_c N_f \int \frac{d^3p}{(2\pi)^3} E_p - 2N_c N_f T \int \frac{d^3p}{(2\pi)^3} [\ln N^+(E_p) + \ln N^-(E_p)], \quad (3)$$

where  $N^+(E_p) = 1 + e^{-\beta(E_p - \mu)}$  and  $N^-(E_p) = 1 + e^{-\beta(E_p + \mu)}$  with  $E_p = \sqrt{\mathbf{p}^2 + m^2}$  and the inverse temperature  $\beta = 1/T$ .

### 1.2. Nambu–Jona-Lasinio model with Polyakov-loop

The deconfinement in pure  $SU(N_c)$  gauge theory can be simulated by introducing an effective potential for a complex Polyakov loop field. The PNJL Lagrangian<sup>10,15–26</sup> is

$$\mathcal{L}_{\text{PNJL}} = \bar{q} (i\gamma_\mu D^\mu - \hat{m}_0) q + G \left[ (\bar{q}q)^2 + (\bar{q}i\gamma_5 \vec{\tau}q)^2 \right] - \mathcal{U}(\Phi[A], \bar{\Phi}[A]; T). \quad (4)$$

Here, the notation is the same as in Eq. (1).

The quark fields are coupled to the gauge field  $A^\mu$  through the covariant derivative  $D^\mu = \partial^\mu - iA^\mu$ . The gauge field is  $A^\mu = \delta_0^\mu A^0 = -i\delta_4^\mu A_4$  (the Polyakov gauge). The field  $\Phi$  is determined by the trace of the Polyakov loop  $L(\vec{x})$ <sup>10</sup>

$$\Phi[A] = \frac{1}{N_c} \text{Tr}_c L(\vec{x}),$$

where  $L(\vec{x}) = \mathcal{P} \exp \left[ i \int_0^\beta d\tau A_4(\vec{x}, \tau) \right]$ .

The gauge sector of the Lagrangian density (4) is described by an effective potential  $\mathcal{U}(\Phi[A], \bar{\Phi}[A]; T)$  fitted to the lattice QCD simulation results in pure  $SU(3)$  gauge theory at finite  $T$ <sup>10,15</sup> with

$$\frac{\mathcal{U}(\Phi, \bar{\Phi}; T)}{T^4} = -\frac{b_2(T)}{2} \bar{\Phi}\Phi - \frac{b_3}{6} (\Phi^3 + \bar{\Phi}^3) + \frac{b_4}{4} (\bar{\Phi}\Phi)^2, \quad (5)$$

$$b_2(T) = a_0 + a_1 \left( \frac{T_0}{T} \right) + a_2 \left( \frac{T_0}{T} \right)^2 + a_3 \left( \frac{T_0}{T} \right)^3. \quad (6)$$

The parameters of the effective potential (5) and (6) are summarized in Table 1.

Table 1. Parameters of the effective potential  $\mathcal{U}[A]$ .

$a_0$	$a_1$	$a_2$	$a_3$	$b_3$	$b_4$
6.75	-1.95	2.625	-7.44	0.75	7.5

The parameter  $T_0$  in general depends on the number of active flavors and the chemical potential<sup>16</sup>. In the present work we use  $T_0 = 270$  MeV as in<sup>10</sup>.

The thermodynamic potential for the PNJL model in the mean-field approximation is given by the following equation<sup>17</sup>

$$\Omega(\Phi, \bar{\Phi}, m, T, \mu) = \mathcal{U}(\Phi, \bar{\Phi}; T) + G \langle \bar{q}q \rangle^2 + \Omega_q, \quad (7)$$

where (in analogy with (2))

$$\Omega_q = -2N_c N_f \int \frac{d^3p}{(2\pi)^3} E_p - 2N_f T \int \frac{d^3p}{(2\pi)^3} [\ln N_\Phi^+(E_p) + \ln N_\Phi^-(E_p)] . \quad (8)$$

Here,  $E_p = \sqrt{\mathbf{p}^2 + m^2}$  is the quark energy,  $E_p^\pm = E_p \mp \mu$ , and

$$N_\Phi^+(E_p) = \left[ 1 + 3 \left( \Phi + \bar{\Phi} e^{-\beta E_p^+} \right) e^{-\beta E_p^+} + e^{-3\beta E_p^+} \right], \quad (9)$$

$$N_\Phi^-(E_p) = \left[ 1 + 3 \left( \bar{\Phi} + \Phi e^{-\beta E_p^-} \right) e^{-\beta E_p^-} + e^{-3\beta E_p^-} \right]. \quad (10)$$

Since NJL-type models are nonrenormalizable it is necessary to introduce a regularization, e.g., by a cutoff  $\Lambda$  in the momentum integration. Following<sup>17</sup>, we use in this study the three-dimensional momentum cutoff for vacuum terms and extend this integration till infinity for finite temperatures. A comprehensive study of the differences between the two regularization procedures (with and without cutoff on the quark momentum states at finite temperature) was performed in<sup>22</sup>.

## 2. Quarks and light mesons in NJL and PNJL models

In the mean-field approximation, we can obtain the constituent quark mass  $m$  from the condition that the thermodynamical potential (Eqs. (2) and (7), resp.) shall have a minimum with respect to varying this parameter,  $\partial\Omega/\partial m = 0$ . This condition is equivalent to the gap equation<sup>14,17</sup>

$$m = m_0 - 2G \langle \bar{q}q \rangle, \quad (11)$$

where the quark condensate is defined as  $\langle \bar{q}q \rangle = \partial\Omega/\partial m_0$ . For the mass gap equation of both models we get

$$m = m_0 + 8GN_c N_f \int_{\Lambda} \frac{d^3p}{(2\pi)^3} \frac{m}{E_p} [1 - f^+ - f^-], \quad (12)$$

with

$$f^+ = (1 + e^{\beta E_p^+})^{-1}, \quad (13)$$

$$f^- = (1 + e^{\beta E_p^-})^{-1} \quad (14)$$

for the NJL model, and

$$f^+ = \left[ \left( \Phi + 2\bar{\Phi} e^{-\beta E_p^+} \right) e^{-\beta E_p^+} + e^{-3\beta E_p^+} \right] / N_{\Phi}^+(E_p), \quad (15)$$

$$f^- = \left[ \left( \bar{\Phi} + 2\Phi e^{-\beta E_p^-} \right) e^{-\beta E_p^-} + e^{-3\beta E_p^-} \right] / N_{\bar{\Phi}}^-(E_p) \quad (16)$$

for the PNJL model. Moreover, for PNJL calculations we should find the values of  $\Phi$  and  $\bar{\Phi}$  by minimizing  $\Omega$  with respect  $\Phi$  and  $\bar{\Phi}$ <sup>17</sup> at given  $T$  and  $\mu$ . One should note, that if  $\Phi \rightarrow 1$ , the expressions Eqs. (15),(16) reduce to the standard NJL model Eqs. (13) and (14).

For a self-consistent description of the particle spectrum in the mean-field approximation, the meson correlations have to be taken into consideration. These correlations are related to the polarization operator of constituent fields. For scalar and pseudoscalar particles the polarization operators are represented by loop-integrals<sup>4,18,19</sup>.

$$\Pi_{ab}^{PP}(P^2) = \int \frac{d^4p}{(2\pi)^4} \text{Tr} [i\gamma_5 \tau^a S(p+P) i\gamma_5 \tau^b S(p)], \quad (17)$$

$$\Pi_{ab}^{SS}(P^2) = \int \frac{d^4p}{(2\pi)^4} \text{Tr} [S(p+P) S(p)], \quad (18)$$

where the operation Tr is taken over Dirac, flavor and color indices of quark fields.

From point of view of the polarization operators, The pseudoscalar ( $\pi$ ) and scalar ( $\sigma$ ) meson masses can be defined by the condition that for  $P^2 = M_{\pi}^2$  ( $M_{\sigma}^2$ ) the corresponding polarization operator  $\Pi^{PP}(M_{\pi}^2)$  ( $\Pi^{SS}(M_{\sigma}^2)$ ), leads to a bound state pole in the corresponding meson correlation function<sup>17</sup>. For mesons at rest

( $\mathbf{P} = 0$ ) in the medium, these conditions correspond to the equations

$$1 + 8GN_c N_f \int \frac{d^3p}{(2\pi)^3} \frac{E_p}{M_\pi^2 - 4E_p^2} (1 - f^+ - f^-) = 0, \quad (19)$$

$$1 + 8GN_c N_f \int \frac{d^3p}{(2\pi)^3} \frac{1}{E_p} \frac{E_p^2 - m^2}{M_\sigma^2 - 4E_p^2} (1 - f^+ - f^-) = 0. \quad (20)$$

In order to solve Eqs. (11), (19) and (20), a set of model parameters has to be determined: the cutoff parameter  $\Lambda$ , the current quark mass  $m_0$  (in chiral limit  $m_0 = 0$ ) and the coupling constant  $G$ . These parameters are fixed at  $T = 0$  to reproduce physical quantities: the pion mass  $M_\pi = 0.139$  GeV, the pion decay constant  $F_\pi = 0.092$  GeV and the quark condensate  $\langle \bar{q}q \rangle^{1/3} = -250$  MeV. The obtained parameters are shown in Table 2.

Table 2. The set of model parameters reproducing observable quantities (in brackets) and the chiral condensate  $\langle \bar{q}q \rangle^{1/3} = -250$  MeV.

$m_0$ [MeV]	$\Lambda$ [GeV]	$G$ [GeV] $^{-2}$	$F_\pi$ [GeV]	$M_\pi$ [GeV]
5.5	0.639	5.227	(0.092)	(0.139)

Solutions of the gap-equation (11) and Eqs. (19), (20) at nonzero  $T$  are presented in Fig. 1. The temperature is normalized to the Mott temperature, which is defined from the condition  $M_\pi(T_{\text{Mott}}) = 2m_q(T_{\text{Mott}})$ . In the PNJL model  $T_{\text{Mott}} \simeq 0.27$  GeV and in the NJL model  $T_{\text{Mott}} \simeq 0.208$  GeV for our parameters. The modification of

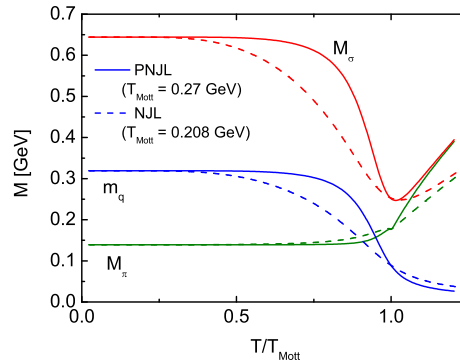


Fig. 1. Temperature dependence of the masses  $m_q$ ,  $M_\pi$  and  $M_\sigma$  at  $\mu = 0$  GeV. Results for PNJL and NJL models are given by the solid and dashed lines, respectively.

the quasiparticle properties is clearly seen in this figure. Up to the Mott temperature  $T_{\text{Mott}}$ , the  $\sigma$  mass practically follows the behaviour of  $2m_q(T)$  with a drop

towards the pion mass signalling chiral symmetry restoration. At  $T/T_{\text{Mott}} > 1$  the masses of chiral partners become equal to each other,  $M_\sigma \approx M_\pi$ , and then both masses increase with temperature. Below the Mott temperature, the pion mass remains practically constant. The transition region from the phase with broken chiral symmetry ( $m_q(T) \sim m_q(0)$ ) to chirally symmetric phase ( $m_q(T) \sim 0$ ) is much narrower in the PNJL case when compared to the NJL model. For a recent discussion of this issue within the nonlocal PNJL model, see <sup>20</sup>.

### 3. Thermodynamics of NJL and PNJL models

The thermodynamics of particles is described in terms of the grand canonical ensemble which is related with the Hamiltonian  $H$  as follows:

$$e^{-\beta V \Omega} = \text{Tr } e^{-\beta(H - \mu N)}, \quad (21)$$

where  $N$  is the particle number operator and the operator  $\text{Tr}$  is taken over momenta as well as color, flavor and Dirac indices. If  $\Omega$  is known, the basic thermodynamic quantities - the pressure, the energy and entropy densities, the density of quarks number and heat conductivity - can be defined as follows:

$$p = -\frac{\Omega}{V}, \quad (22)$$

$$s = -\left(\frac{\partial \Omega}{\partial T}\right)_\mu, \quad (23)$$

$$\varepsilon = -p + Ts + \mu n, \quad (24)$$

$$n = -\left(\frac{\partial \Omega}{\partial \mu}\right)_T, \quad (25)$$

$$c = \frac{T}{V} \left(\frac{\partial s}{\partial T}\right)_\mu. \quad (26)$$

The thermodynamic potential in equilibrium corresponds to a global minimum with respect to variations of the order parameter(s)

$$\frac{\partial \Omega(T, \mu, m)}{\partial m} = 0, \quad \frac{\partial^2 \Omega(T, \mu, m)}{\partial m^2} \geq 0. \quad (27)$$

All these relations describe thermodynamics of the system. For the considered models the thermodynamic potentials are defined from Eqs. (2) and (7). From these equations we can read off the vacuum part

$$\Omega_{vac} = \frac{(m - m_0)^2}{4G} - 2N_c N_f \int \frac{d^3 p}{(2\pi)^3} E_p. \quad (28)$$

This quantity does not vanish at  $T \rightarrow 0$  and  $\mu \rightarrow 0$ . Therefore, in order to obtain the physical thermodynamical potential which corresponds to vanishing pressure and energy density at  $(T, \mu) = (0, 0)$ , one has to renormalize the thermodynamic potential by subtracting its vacuum expression (28). This corresponds to the following

definition of the physical pressure

$$\frac{p}{T^4} = \frac{p(T, \mu, m) - p(0, 0, m)}{T^4}. \quad (29)$$

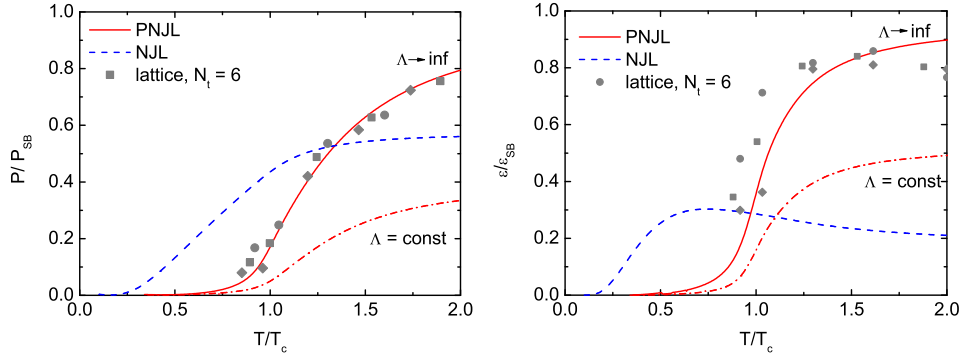


Fig. 2. The temperature dependence of the reduced pressure and energy density within the PNJL model for  $\mu = 0$  in two schemes of regularization  $\Lambda = 0.639$  and  $\Lambda \rightarrow \infty$ . Dotted lines are appropriate results for the NJL model. Lattice data points for  $N_f = 2$  at  $\mu = 0$  are from Ref. [27]. Circles, squares and diamonds correspond to calculations at  $N_t = 6$  with the mass ratio of the pseudoscalar to vector meson  $m_{PS}/m_V = 0.65, 0.70$  and  $0.75$ , respectively.

Within the PNJL model with  $\Lambda \rightarrow \infty$  the reduced pressure and energy density exhibit reasonable behavior consistent with the recent lattice QCD results for the vanishing chemical potential<sup>27</sup> (see Fig. 2) keeping in mind that the  $m_{PS}/m_V$  ratio in lattice calculations is still far from that for physical masses  $m_{PS}/m_V \sim 0.2$ . One should note that both models have the cutoff parameter  $\Lambda$ <sup>17</sup>. But the integrals containing the logarithm in Eq. (2) and Eq. (7) are both convergent<sup>10,25</sup>. In our work we calculated these integrals with  $\Lambda \rightarrow \infty$ . It leads to the flattening of pressure at high temperature. However, most integrals for the PNJL model are convergent too. This was the reason to consider the thermodynamic functions for  $\Lambda \rightarrow \infty$ . It was supposed that with increasing temperature the pressure has to reach the Stefan-Boltzmann limit<sup>22</sup>, which in the PNJL model is defined as

$$\frac{p_{SB}}{T^4} = (N_c^2 - 1) \frac{\pi^2}{45} + N_c N_f \frac{7\pi^2}{180} \simeq 4.053. \quad (30)$$

If the regularization  $\Lambda = 0.639$  is used, the  $T$ -behaviour of the thermodynamic quantities considered is roughly the same while their absolute values are noticeably lower, being far from the Stefan-Boltzmann limit. In the NJL model both,  $p/T^4$  and  $\varepsilon/T^4$  are not only underestimated due to the missing gluon contribution, but also essentially shifted toward lower temperatures because of the lack of a confining mechanism for the dynamical quark degrees of freedom.

Within NJL-like models there are several characteristic temperatures. The parameter  $T_0$  entering the effective potential (6) of the PNJL model has been noted

above. Three other scales are the pseudo-critical temperature for chiral crossover  $T_\chi$  defined by the maximum of  $\partial\langle q\bar{q}\rangle/\partial T$ , the pseudo-critical temperature for the deconfinement crossover  $T_p$  which can be found from the maximum of  $\partial\bar{\Phi}/\partial T$ , and  $T_c$  defined for PNJL model as the average of two transition temperatures  $T_\chi$  and  $T_p$ <sup>10,15</sup>. The temperature dependence of the order parameters for the chiral ( $\langle q\bar{q}\rangle$ ) and deconfinement ( $\Phi$ ) phase transitions, are shown in Fig. (3). The chiral condensate decreases and the Polyakov loop potential increases with  $T$ , demonstrating closeness of the pseudo-critical temperatures  $T_\chi$  and  $T_p$  at  $\mu = 0$  (see also Table 3). For  $\pi$ -mesons, the Mott temperature  $T_{\text{Mott}}$  is provided by the condition

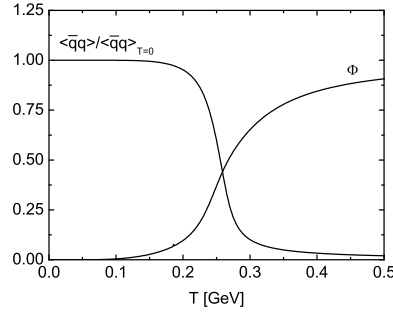


Fig. 3. Temperature dependence of the chiral condensate and Polyakov loop potential at  $\mu = 0$  GeV within the PNJL model

$M_\pi(T_{\text{Mott}}) = 2m_q(T_{\text{Mott}})$  and similarly the  $\sigma$  meson dissociation temperature  $T_d^\sigma$  is given by the equation  $M_\sigma(T_d^\sigma) = 2M_\pi(T_d^\sigma)$ <sup>19,21</sup>. All these quantities obtained at  $\mu = 0$  are presented in Table 3.

Table 3. Characteristic temperatures in NJL and PNJL models.

	$T_0$	$T_\chi$	$T_p$	$T_c$	$T_{\text{Mott}}$	$T_d^\sigma$
NJL	–	0.192	–	0.192	0.207	0.185
PNJL	0.27	0.249	0.258	0.253	0.27	0.259

Extending our study of the (pseudo-)critical temperatures to nonzero chemical potential  $\mu$ , we obtain phase diagrams in the  $T - \mu$  plane shown in Fig. 4. The chiral transition line, determined by<sup>4</sup>

$$\left[ \frac{1}{4G} + \frac{\partial\Omega_q}{\partial m^2} \right]_{m=0} = 0$$

in both NJL and PNJL models, is a monotonously decreasing function of the chemical potential. In the limiting chirally symmetric case corresponding to  $m = 0$  the  $T_\chi$  at large  $\mu$  is higher than those for finite mass but both temperatures coincide



when  $\mu \rightarrow 0$  for both the NJL and PNJL models. For the case  $\mu \neq 0$  both models show the critical end point at the temperature  $T_{CEP}$  below which the chiral phase transition is of first order. At this point  $(T_{CEP}, \mu_{CEP})$  the phase transition changes from first order to crossover<sup>22,23,24</sup>. For the chirally symmetric case in the PNJL model the first order phase transition ends at a tricritical point above which, for  $T > T_{TCP}$ , the chiral transition is of the second order. In the NJL model<sup>28</sup> the topology of the phase diagram is the same as in the PNJL case, only  $T_{CEP}$  and  $T_{TCP}$  are situated at higher temperatures. In accordance with other calculations, the temperature of the tricritical point is above that of the critical end point. Within the PNJL model the positions of critical points are  $(T_{CEP}, \mu_{CEP}) = (95, 320)$

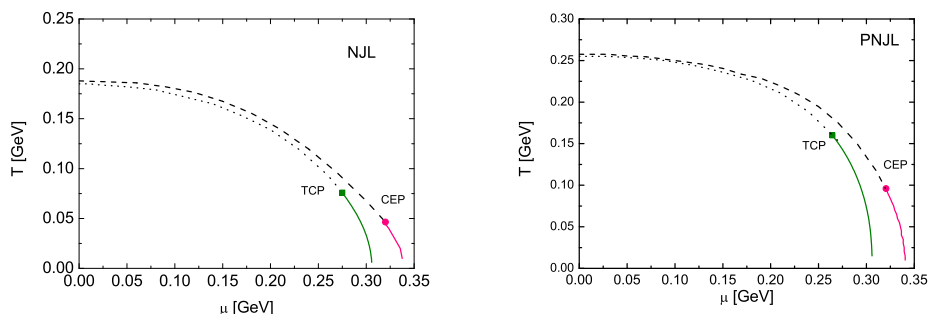


Fig. 4. Phase diagrams of NJL (left panel) and PNJL (right panel) models. Solid lines correspond to the first order phase transition, dashed lines are crossover and dotted lines are the boundary of the second order phase transition.

and  $(T_{TCP}, \mu_{TCP}) = (160, 265)$  MeV. These numbers are quite close to those in<sup>22</sup> for the set with similar parameter values (set B, the case I). One should emphasize that critical properties of observables are significantly influenced by the chosen parameter set and regularization procedure as was demonstrated in<sup>22</sup>.

#### 4. Conclusion

We have compared the thermodynamics of NJL and PNJL models. In agreement with previous results, it is shown that the inclusion of coupling between chiral symmetry and deconfinement essentially improves the description of thermodynamic bulk properties of the medium. The models qualitatively reproduce both,  $\pi$  and  $\sigma$  meson properties in hot, dense quark matter and the rich and complicated phase structure of this medium. Effects of the Polyakov loop move the CEP to higher  $T$  and lower  $\mu$  than in the NJL case<sup>15</sup>. The position of the calculated CEP in the  $T - \mu$  plane is still far from the predictions of lattice QCD and empirical analysis. The further elaboration of the presented models may include color superconducting phases and nonlocality of the interaction<sup>29</sup> as well as effects beyond the meanfield<sup>30</sup>.

## Acknowledgments

We are grateful to D. Blaschke, P. Costa and V. V. Skokov for useful comments. V.T. acknowledges financial support from the Helmholtz International Center (HIC) for FAIR within the LOEWE program. The work of Yu. K. was supported by RFFI grant No. 09-01-00770a.

## References

1. Y. Nambu and G. Jona-Lasinio, Phys. Rev. **122**, 345 (1961).
2. M. K. Volkov, Annals of Physics **157**, 282 (1984).
3. U. Vogl and W. Weise, Progr. Part. Nucl. Phys. **27**, 195 (1991).
4. S. P. Klevansky, Rev. Mod. Phys. **64**, 649 (1992).
5. T. Hatsuda and T. Kunihiro, Phys. Rep. **27**, 221 (1994).
6. M. Buballa, Phys. Rep. **407**, 205, (2005).
7. M. K. Volkov and A. E. Radzhabov, Phys. Usp. **49**, 551 (2006).
8. P. N. Meisinger, T. R. Miller, and M. C. Ogilvie, Phys. Rev. **D 65**, 034009 (2002).
9. K. Fukushima, Phys. Lett. **B 591**, 277 (2004).
10. C. Ratti, M. A. Thaler and W. Weise, Phys. Rev. **D 73**, 014019 (2006).
11. E. Megias, E. Ruiz Arriola and L. L. Salcedo, Phys. Rev. **D 74**, 065005 (2006).
12. S. K. Ghosh, T. K. Mukherjee, M. G. Mustafa and R. Ray, Phys. Rev. **D 73**, 114007 (2006).
13. M. Asakawa and K. Yazaki, Nucl. Phys. **A 504**, 668 (1989).
14. J. Hüfner, S. P. Klevansky and P. Zhuang, Acta Phys. Pol. **B 25**, 85 (1994).
15. S. Rössner, C. Ratti and W. Weise, Phys. Rev. **D 75**, 034007 (2007).
16. B. J. Schaefer, J. M. Pawłowski and J. Wambach, Phys. Rev. **D 76**, 074023 (2007).
17. H. Hansen, W. M. Alberico, A. Beraudo, A. Molinari, M. Nardi and C. Ratti, Phys. Rev. **D 75**, 065004 (2007).
18. H. J. Schulze, J. Phys. **G 21**, 185 (1995).
19. E. Quack, P. Zhuang, Y. Kalinovsky, S. P. Klevansky and J. Hüfner, Phys. Lett. **B 348**, 1 (1995).
20. D. Horvatic, D. Blaschke, D. Klabucar and O. Kaczmarek, arXiv:1012.2113 [hep-ph].
21. W. J. Fu and Y. X. Liu, Phys. Rev. **D 79**, 074011 (2009).
22. P. Costa, M. C. Ruivo, H. Hansen and C. A. de Sousa, Phys. Rev. **D 81**, 016007 (2010).
23. K. Kashiwa, H. Kuono, M. Matsuzaki and M. Yahiro, Phys. Lett. **B 662**, 26 (2008).
24. K. Fukushima, Phys. Rev. **D 78**, 114019 (2008).
25. C. Sasaki, B. Friman and K. Redlich, Phys. Rev. **D 75**, 054026 (2007).
26. Z. Zhang and Y. X. Liu, Phys. Rev. **C 75**, 064910 (2007).
27. A. Ali Khan et al., Phys. Rev. **D64**, 074510 (2001).
28. O. Scavenius, A. Mocsy, I. N. Mishustin and D. H. Rischke, Phys. Rev. **C 64**, 045202 (2001).
29. D. Gomez Dumm, D. B. Blaschke, A. G. Grunfeld, N. N. Scoccola, Phys. Rev. **D73**, 114019 (2006).
30. D. Blaschke, M. Buballa, A. E. Radzhabov, M. K. Volkov, Yad. Fiz. **71**, 2012-2018 (2008).